Most hippocampal CA1 pyramidal cells in rabbits increase firing during awake sharp-wave ripples and some do so in response to external stimulation and theta

Running head: CA1 activity during conditioning

Miriam S. Nokia[1*], Tomi Waselius[1], Joonas Sahramäki[1] & Markku Penttonen[1]

[1]Department of Psychology, University of Jyväskylä, Jyväskylä, Finland

*corresponding author: miriam.nokia@jyu.fi, P.O. Box 35, 40014, University of Jyväskylä

Acknowledgements

We thank Irina Gureviciene, Henriikka Huhtamäki and Eveliina Pöllänen for their contribution to data acquisition. We also thank Lauri Kantola, Arto Lipponen and Tiina Pirttimäki for help with data analysis and Jan Wikgren and Heikki Tanila for advice on the study design. We thank the following people for their advice on single-unit recordings and data analysis: Francesco Battaglia, Jozsef Csicsvari, Ronny Eichler, Joseph O'Neill and Tim Schröder. This work was supported by the Academy of Finland (grant ns. 275954 and 286384 to MSN, 316966 to MP). The authors declare no conflict of interests.

Abstract

Hippocampus forms neural representations of real-life events including multimodal information of spatial and temporal context. These representations, i.e. organized sequences of neuronal firing are repeated during following rest and sleep, especially when so-called sharp-wave ripples (SPW-Rs) characterize hippocampal local-field potentials. This SPW-R – related replay is thought to underlie memory consolidation. Here, we set out to explore how hippocampal CA1 pyramidal cells respond to the conditioned stimulus during trace eyeblink conditioning and how these responses manifest during SPW-Rs in awake adult female New Zealand White rabbits. Based on reports in rodents, we expected SPW-Rs to take place in bursts, possibly according to a slow endogenous rhythm. In awake rabbits, half of all SPW-Rs took place in bursts, but no endogenous slow rhythm appeared. Conditioning trials suppressed SPW-Rs while increasing theta for a period of several seconds. As expected based on previous findings, only a quarter of the putative CA1 pyramidal cells increased firing in response to the conditioned stimulus. Compared to other cells, rate increasing cells were more active during spontaneous epochs of hippocampal theta while response profile during conditioning did not affect firing during SPW-Rs. Taken together, CA1 pyramidal cell firing during SPW-Rs is not limited to cells that fired during the preceding experience. Further, the importance of possible reactivations taking place during theta epochs on memory consolidation warrants further investigation.

Keywords

hippocampus, theta, sharp-wave ripple, classical conditioning, pyramidal cell

New & Noteworthy

We studied hippocampal sharp-wave ripples, theta and CA1 pyramidal cell activity during trace eyeblink conditioning in rabbits. Conditioning trials suppressed ripples while increasing theta for a period of several seconds. A quarter of the cells increased firing in response to the conditioned stimulus and fired extensively during endogenous theta as well as ripples. The role of endogenous theta epochs in off-line memory consolidation should be studied further.

Introduction

Hippocampal neuronal activity is involved in forming new episodic memories (Scoville and Milner 1957; Lisman et al. 2017), especially in encoding of location and time or the context of events. So-called place cells, i.e. cells that fire in a certain location, were characterized in the rat hippocampus almost 50 years ago (O'Keefe and Dostrovsky 1971). In addition, cells that fire in sequences during idle wait periods have been reported in the rat hippocampal CA1 and are sometimes referred to as time cells (MacDonald et al. 2011; MacDonald et al. 2013; Mau et al. 2018; Pastalkova et al. 2008). Whether reflecting spatial or temporal information, the sequences of neuronal activation that take place in the hippocampus during experiences are known to be replayed and pre-played during quiet immobility (Foster and Wilson 2006; Tang et al. 2017; Wu et al. 2017) and slow-wave sleep (Buzsaki 2015; Wilson and McNaughton 1994). This synchronous firing of CA1 pyramidal cells is manifested in the hippocampal CA1 local-field potentials (LFPs) of mammals as so-called sharp-wave ripples (SPW-Rs, 80-250 Hz) (Buzsaki 2015; Ylinen et al. 1995).

In rodents, SPW-Rs tend to occur in bursts (Oliva et al. 2018; Yamamoto and Tonegawa 2017), and neocortical slow oscillations modulate the occurrence of SPW-Rs (Headley et al. 2017; Sirota et al. 2003). The emergence of SPW-Rs is regulated also by input arriving from sub-cortical structures (see Logothetis et al. 2012). Interestingly, SPW-R probability is increased during nasal expiration in mice (Liu et al. 2017) which suggests a possibility for a slow rhythmicity in their occurrence (see also Klimesch 2018; Penttonen and Buzsaki 2003; Penttonen et al. 1999). Within the hippocampus, SPW-Rs are thought to originate in the CA3 pyramidal cells (Buzsaki 1986) but recent findings also suggest a role for the CA2 (Oliva et al. 2016) and dentate gyrus (Sasaki et al. 2018). SPW-Rs are proposed to reflect “off-line” memory consolidation (Buzsaki 1989, 2015). Indeed, experimental evidence indicates both awake (Jadhav et al. 2012; Nokia et al. 2012a) and sleep-state SPW-

Rs (Girardeau et al. 2009; Maingret et al. 2016; Novitskaya et al. 2016) are critical for memory formation, possibly due to information exchange between the hippocampus and the neocortex during and around them. In conclusion, SPW-Rs seem crucial for effective cognition.

Another hippocampal oscillatory phenomenon related to learning is theta (Buzsáki 2002), a rhythmic slow oscillation that in rabbits has a frequency of around ~6 Hz which in rodents corresponds to type 2 theta (~4-8 Hz) dependent on acetylcholine signaling. Type 2 theta rhythm originates in the medial septum - diagonal band of Broca and has been associated to arousal and alertness while the animal is quietly orienting towards the outside world (Buzsáki 2002). In immobile animals, epochs of dominant hippocampal theta occur both endogenously as well as exogenously in response to external stimulation, such as classical trace eyeblink conditioning (TEBC) (rabbits: Nokia et al. 2009; rats: Nokia et al. 2012b). The degree, to which external stimulation elicits coherent theta oscillations and adaptive behavior change seems to depend on the neural state preceding stimulus onset (Griffin et al. 2004; Nokia and Wikgren 2014; Nokia et al. 2015). Whether endogenously generated theta oscillations in awake immobility also contribute to memory consolidation after the initial experience, is uncertain.

Here, to probe CA1 pyramidal cell firing related to learning beyond the context of spatial exploration and place cells, we studied adult female New Zealand White rabbits during hippocampus-dependent TEBC (Kim et al. 1995; Takehara et al. 2002). First, we sought to find out if SPW-Rs recorded during TEBC conducted in a restrainer differ from those recorded during free movement and rest without any external stimulation. Second, we studied if the SPW-Rs take place in bursts and whether their occurrence is rhythmic. Third, we explored how CA1 pyramidal cells respond to the conditioned stimulus (CS) used for TEBC. Based on a previous report (Hattori et al. 2015) we expected only a small fraction of

CA1 pyramidal cells to increase firing in response to the CS. At last, we examined the firing of CA1 pyramidal cells during the inter-trial intervals. Our assumption was that cells possibly encoding the features of the CS on-line (rate increasing) would also preferably fire during awake SPW-Rs. This could be interpreted to reflect memory consolidation off-line (Buzsaki 1989, 2015).

Methods and materials

Ethical permit

All the experimental procedures, care and handling were executed in accordance with Directive 2010/63/EU of the European Parliament and of Council on the protection of animals used for scientific purposes. Permission to conduct the experiment was obtained from the Animal Experiment Board in Finland working under the Regional State Administrative Agency (ESAVI/6718/04.10.07/2015).

Subjects

The subjects were six adult female New Zealand White rabbits (Lidköpings kaninfarm, Sweden) weighing approximately 2.8 kg at the time of surgery. The rabbits were housed in individual cages at the Laboratory center of the University of Jyväskylä. Food and water were freely available, and room temperature and humidity were controlled. The rabbits were maintained on a 12/12-h light/dark cycle, with lights on at 8:00 a.m. All experiments were carried out during the light part of the cycle. Animal handling was performed only by trained personnel and the rabbits were introduced to human contact and handling before the surgery.

Surgery

Before the surgery, rabbits were treated with subcutaneous injections (s.c.) of an anti-inflammatory drug (50 mg/mL carprofen [Rimadyl vet, Pfizer Inc. Animal Health], dose: 0.1 mL/kg) and with 2 ml of an analgesic drug (buprenorphine, dose 0.03 mg/kg, concentration 0.03 mg/mL; Temgesic [Schering-Plough Europe]) to moderate acute pain after surgery. The rabbits were anesthetized with an intramuscular injection (i.m.) of ketamine–xylazine cocktail (7.8 ml of 50 mg/mL Ketaminol vet [Intervet International B.V.] mixed with 2.8 ml of 20 mg/mL Narcoxyl vet [Intervet International B.V.]). A dose of 0.8 mL/kg of the cocktail was

injected i.m. before surgery. During surgery, additional doses of either the cocktail or ketamine alone were injected subcutaneously approximately every 20–30 min or as needed. Before the surgery, the rabbit's fur was shaved from the top of the head. Then, the rabbit was positioned in a stereotaxic instrument (Kopf Instruments) with the bregma 1.5 mm higher than the lambda. Eye gel was applied to prevent the rabbit's eyes from drying during surgery. At this point, 2.0 ml of lidocaine (10 mg/mL Lidocain [Orion pharma]) was injected s.c. in the area of surgery before making the opening incision.

A longitudinal incision was made to the scalp and a local anesthetic (2 g of lidocaine-hydrochloride Xylocain [AstraZeneca]) was administered to the wound. Four holes for the anchoring screws were drilled bilaterally at 5 mm anterior and 5 mm lateral to the bregma and at 13 mm posterior and 5 mm lateral to the bregma. The two posterior and the two anterior screws were connected together and served as a reference (posterior pair) and the ground (anterior pair) for the electrophysiological recordings. Next, a craniotomy was made over the right dorsal hippocampus at 4-6 mm posterior and 4-7 mm lateral from the bregma. Dura was removed and a silicone probe with 4 shanks each with 8 electrodes (E32B-20-S04-L10.0-200 with a pointy tip, Atlas Neuroengineering) attached to a microdrive (nDrive xL, NeuroNexus) was lowered in place, aiming at 1 mm above the CA1 pyramidal layer. Kwik-Sil (World Precision Instruments) silicone was used to seal the craniotomy. The microdrive and the probe were shielded with a plastic covering. Wires, skull screws, preamplifier interface, one mounting screw for an air puff mount, and the incision area were covered with dental acrylic. To prevent nausea after surgery, metoclopramide (0.1 mL/kg, concentration 5 mg/mL; Primperan [Sanofi Winthrop Industrie]) was administered s.c. and the rabbit was returned to its home cage wrapped in a towel. Recovery was monitored and the rabbits were medicated with s.c. injections of buprenorphine (0.03 mg/kg, concentration 0.03 mg/mL; Temgesic [Schering-Plough Europe]) 4 h after surgery and then every 8 h for the next 44 h.

Behavioral training and recordings

LabVIEW (National Instruments) was used to monitor neural activity and blinking online, to execute the experimental procedures and to present stimuli.

Trace eyeblink conditioning

After one week of recovery from surgery, the animals were accustomed to a Plexiglas restraining box and overall behavior was monitored. On the second day, restrained animals were habituated to the recording chamber for 30 min. On the next day, during the first training session, 60 tone-alone (200-ms, 5-kHz, 75-dB tone) trials were presented. The inter-trial interval always varied between 30 and 60 s. Then, on consecutive days, trace eyeblink conditioning was carried out with the tone specified above as the conditioned stimulus (CS) and a 100-ms air puff (0.35 bar source pressure) to the right eye as an unconditioned stimulus (US). A silent trace period of 500 ms separated the offset of the CS from the onset of the US. Once the animals had acquired a robust learned response, the trace period was lengthened from 500 ms to 1000 ms and training continued. This was done because our aim was to record CA1 pyramidal cells throughout both training phases to allow for within-subject comparisons between the short and long trace periods. A total of 60 training trials were presented during each session, in the absence of spontaneous blinking. After each session, a subset of animals (n = 4) was let to rest for 1 hour in a quiet room with dim lighting in a cage identical to home cage. Then the animals were returned to home cage.

Recording

Neural signals and electromyography (EMG) from the right eye were recorded 5 min prior to, during and 1 min after each TEBC session. Bipolar EMG from the trained eye was recorded using stainless steel wire-hooks placed around the right upper and lower eyelids for the duration of the training sessions. The raw EMG signal was conveyed to a filter-amplifier (A-M Systems Model 2100), amplified 1000x and band-pass filtered from 100 to 500 Hz. For

neural recordings, the silicone probe was connected to a wireless preamplifier (W2100-HS32, MultiChannel Systems [MCS]). The signals were band-pass filtered (1–5000 Hz) and digitized and stored at a rate of 20 kHz with a MCS wireless recording system (W2100, Mc_Rack software). For a subset of animals (n = 4) neural signals were also recorded during a 1-hr rest session following the TEBC session, but in these recordings the signal quality was lower (possibly due to the cage structure) and only allowed analysis of local-field potentials.

Histology

When all experimental procedures were finished, the animals were anesthetized with an i.m. injection of ketamine-xylazine cocktail and then overdosed with an i.v. injection of pentobarbital (Mebunat vet, Orion-Yhtymä Oyj, Espoo, Finland). Next, the brain was perfused with physiological saline followed by 9% formalin solution through the ascending aorta. The locations of the electrode tips were marked by passing a DC current (200 µA, 20 s) through them. The brain was then removed and stored in formalin for several days. Next, the brain was coronally sectioned with a vibratome into 40-µm-thick slices. The slices were attached to slides, dried and stained with cresyl violet. The electrode-tip locations were determined with the help of a microscope.

Data analysis

MATLAB (MathWorks), python and SPSS (IBM) were used for offline data analysis.

Trace eyeblink conditioning

Using custom-made scripts in MATLAB, the EMG signal was high-pass filtered offline (>100 Hz) and Hilbert-transformed. An envelope curve following the peaks of the signal was calculated. Baseline EMG activity was defined for each animal and session as the mean of the peak EMG amplitude during a 250-ms pre-CS period (MEANpre). In addition, the mean of the standard deviation of the EMG activity during the 250-ms pre-CS period

(SDpre) was determined. Eyeblinks were defined as EMG activity exceeding a threshold of [MEANpre + 7 × SDpre] for at least 10 ms. Trials with eyeblinks during the 100-ms period immediately preceding CS onset were rejected. Eyeblinks during the last 250 ms of the trace period were counted as learned responses. The percentage of learned responses per animal per session was used to determine learning. A percentage higher than 80 was used as the criterion for learning. For analyzing data in the early and late stages of learning we used a cut-off value of 50 % learned responses within a session.

Single-units

Recordings were converted from a MultiChannel Systems file format to a raw binary file and the channel order was remapped to accurately represent the electrode contact configuration in the silicon probe. The raw binary file was then fed to *Kilosort* (https://github.com/cortex-lab/KiloSort) for filtering, spike detection, feature extraction and finally, spike sorting. The results of the automatic clustering were inspected and manually curated with *phy* (https://github.com/cortex-lab/phy). Well-separated units were classified as pyramidal cells (pyr) based on overall firing rate and spike waveform. Units with an overall firing rate less than 10 Hz and a trough-to-peak -interval longer than 0.25 ms were classified as putative pyramidal cells (Ranck 1973). For the sake of clarity, we treated all units recorded at different time points as independent cells, although it is possible that some cells were recorded multiple times. To determine possible rate increase or decrease in response to the tone-stimulus used as a conditioned stimulus during TEBC (Hattori et al. 2015), we compared firing (10-ms bins) of each unit during a 700-ms baseline period and a 700-ms response period starting at the CS onset with paired samples t-test. We chose this time period for analysis because for making the association between the CS and the US, a memory trace of the CS must be maintained throughout the trace period, and it is possible that this is reflected in the hippocampal neuronal firing. Note that in a previous report (Hattori et al.

2015) the increase in eyeblinks during the trace period as a result of learning did not affect the response profiles of the CA1 (rate increasing) pyramidal neurons. Thus, for the sake of comparability, we chose to use the same response period throughout our experiment, also during recordings where the US started a full second after the CS offset (see Figure 3).

Local-field potentials

To extract epochs of theta oscillations from the CA1 LFP, segments with a high theta ratio, i.e. high relative power at the 4-8 Hz band, were detected using custom MATLAB scripts (see Nokia et al. 2008). Note that we analyzed only theta epochs that took place > 10 s after the CS onset. These epochs were thought to reflect purely endogenous theta. The phase of the theta-band LFP was determined using the Hilbert transform followed by the angle-command in Matlab. Then each spike that had taken place during a high-theta epoch was assigned the corresponding theta phase value and the firing rate per unit plotted against the phase of the theta oscillation. Phase preference was analyzed using a Circular Statistics Toolbox for Matlab available online: https://se.mathworks.com/matlabcentral/fileexchange/10676-circular-statistics-toolbox-directional-statistics (Berens 2009). Specifically, we used the functions 'circ_mean' and 'circ_rtest' to determine whether a cell fired preferably at a certain phase. The first function gives the mean direction or angle of the resultant vector and the second function tests for non-uniformity of firing.

To detect hippocampal SPW-Rs from the CA1 LFP, the signal was filtered between 80-250 Hz and the envelope of the band-passed LFP was derived using the Hilbert transformation. Next, the mean (M) and the standard deviation (SD) for the envelope were determined. SPW-Rs were detected when the envelope exceeded a threshold of M + 5 * SD. The SPW-R center was determined as the trough of the deepest negative deflection in the band-pass filtered signal. From here on, we will refer to this point as the ripple trough. The

ripple amplitude was determined as the magnitude of the largest positive peak relative to a threshold of mean + 3 * standard deviation. Note that to avoid double-classification at least 100 ms had to elapse from the previous ripple trough to begin searching for another SPW-R. Next, the number of cycles and the exact ripple frequency were determined. Only SPW-Rs with a ripple frequency of 80 Hz or above and at least 3 cycles were kept for further analysis of SPW-R properties and bursts of SPW-Rs. SPW-R bursts were defined as clusters of SPW-Rs in which the interval between adjacent SPW-R maximums was less than 500 ms.

Note that for analyzing single-unit activity related to SPW-Rs, all events detected by the simple thresholding were used. SPW-R -modulation of single units was evaluated similar to Jadhav and colleagues (Jadhav et al. 2012). Briefly, a set of surrogate data (n = 5000) was created by introducing random jitter to the ripple trough -triggered sweeps. Note that the spikes taking place during a given SPW-R were all shifted by the same amount of time to maintain the structure of the firing sequence within a given SPW-R. Then, the Peri-Stimulus Time Histogram (PSTH) around the ripple trough was calculated and compared to the mean PSTH calculated from the surrogate data set: Namely, the squared difference between the real SPW-R-PSTH and the mean of the surrogate PSTHs was obtained. The same was done for the individual surrogate PSTHs (n = 5000). Then, the modulation measure was calculated as the mean at -100 to 100 ms around the ripple trough. If this measure of the real SPW-R-PSTH was greater than 99.9% of that of the surrogate PSTHs (that is, $p < 0.001$), the firing of that neuron was determined to be modulated by SPW-Rs. The firing rate of each unit during the SPW-R (-100 ms to 100 ms relative to the ripple trough) was determined. The latency of the peak in firing was defined by first smoothing the PSTH using a 25-ms window (Savitzky-Golay method) and then finding the peak of the smoothed PSTH within 100 ms from the ripple trough. Note that units with fewer than 30 spikes during all the detected SPW-Rs during a single recording session were excluded from further analysis of SPW-Rs. Firing in

relation to ripple phase was determined similar to how it was done for theta, using the Circular Statistics Toolbox for Matlab (Berens 2009).

Statistics

One-way ANOVA and paired samples t-test were used when appropriate. Bonferroni correction was used in post-hoc comparisons. Correlations were calculated using Pearson's correlation coefficient. Autocorrelations were calculated in MATLAB using the autocorr – function and statistical significance was evaluated based on 95% confidence bounds. Phase preference was analyzed with the toolbox by Berens (2009), and cells were categorized as having a non-uniform firing profile if the Rayleigh test p-value was below 0.001.

Data availability statement

The data that support the findings of this study are available from the corresponding author upon reasonable request.

Results

All rabbits learned trace eyeblink conditioning

All of the animals acquired a robust learned response during TEBC using the 500-ms trace period (Figure 1A) and half of the rabbits also mastered the task when the trace interval was increased to 1000 ms (Figure 1B). The grand average learning curves are depicted in Figure 1C.

SPW-Rs in awake rabbits occurred in bursts and were similar during TEBC sessions and free rest sessions

First, we aimed to find out if SPW-Rs recorded during TEBC conducted in a restrainer differ from those recorded during free movement and rest without any external stimulation. Histological examination confirmed that in all rabbits the recording electrode had

been placed in the hippocampus (Figure 2A). Examples of SPW-Rs recorded from the CA1 in one rabbit are depicted in Figure 2 panels B and D. Altogether 100 recordings from freely moving resting conditions similar to homecage, and 247 recordings from awake restrained state were analyzed for SPW-R characteristics. SPW-R rate [Mean ± Standard Error of Mean (SEM): 16.7 ± 0.3 per minute], frequency (131.8 ± 0.8 Hz), relative amplitude (1.77 ± 0.0 a. u.) and number of cycles (6.0 ± 0.0) were all positively correlated with each other (all 347 sessions from six animals, $r = 0.361 – 0.861$, $p < 0.001$). That is, overall, the more often SPW-Rs took place, the faster, larger and longer they were.

As evident from Figure 2B, SPW-Rs in awake rabbits took place in bursts. Thus, we defined bursts as groups of SPW-Rs in which the interval between adjacent SPW-Rs was less than 500 ms. Within 316 recordings analyzed, on average 51.6 ± 0.48 % of SPW-Rs were singlets, 26.1 ± 0.23 % belonged to doublets, 11.8 ± 0.18 % to triplets and 10.4 ± 0.30 % to longer bursts (see Yamamoto and Tonegawa 2017).

To compare the properties of SPW-Rs between restrained and freely moving state using paired samples t-test, we used data from the four rabbits that had been recorded during TEBC and then during rest (97 paired sessions). Ripples took place on average 17.2 ± 0.4 times per minute during TEBC and 18.0 ± 0.4 time per minute during free rest, $t (96) = 1.61$, $p = 0.111$, 95 % Confidence Interval [-1.76, 0.19]. There was no difference in SPW-R bursts recorded during TEBC and those recorded during rest (one-way ANOVA, $F [1, 314] = 0.048 – 1.534$, $p = 0.217 – 0.826$) (Figure 2C). Ripples recorded during rest were slightly slower in frequency compared to those recorded during TEBC training: 131.5 ± 1.5 Hz vs. 134.0 ± 1.8 Hz, $t (96) = 3.12$, $p = 0.002$, 95 % CI [0.92, 4.11]. There were on average 6 cycles per ripple in both conditions, $t (96) = 1.98$, $p = 0.051$, 95% CI [0.00, 0.21]. There was no significant difference between the two conditions in ripple amplitude, $t (96) = 1.47$, $p = 0.145$, 95 % CI

[-0.01, 0.05]. To summarize, SPW-Rs were similar during TEBC sessions and free rest sessions.

To examine whether SPW-R properties were connected to the performance of the learned response, we correlated the percentage of learned responses with SPW-R occurrence rate (per minute), ripple frequency (Hz), number of cycles and relative amplitude in each rabbit separately. No consistent correlations were found (data not shown).

SPW-Rs and theta epochs time-locked to external stimuli but showed no endogenous slow rhythmicity

Next, we analyzed the possible rhythmicity in the occurrence of SPW-Rs. The probability of an SPW-R was low right after the training trial and reached a plateau at ~10 s after the tone onset (Figure 2E, see also Nokia et al. 2012a). To examine endogenous rhythmicity, we calculated PSTHs of the SPW-R occurrences recorded during the stimulus-free rest sessions. Autocorrelograms (maximum delay 60 s) indicated no statistically significant peak values at a delay greater than 5 seconds indicating no innate slow rhythmicity in SPW-Rs (see Figure 2F). In sum, SPW-Rs did not occur rhythmically but were time-locked to external stimulation.

For comparison, also the timing of theta epochs is illustrated in Figure 2. As evident, contrary to SPW-Rs, theta epochs were most abundant immediately following the training trials (Fig. 2E). Similar to the SPW-Rs, there was no slow rhythmicity observed (Fig. 2F).

Only a minority of CA1 pyramidal cells increased firing rate in response to the conditioned stimulus

In addition to examining SPW-Rs, our aim in this research was to study the response profiles of hippocampal CA1 pyramidal cells during a non-spatial associative task. Earlier reports indicate most CA1 pyramidal cells do not increase firing rate in response to the

conditioned stimulus, and that the firing properties remain similar across training (Hattori et al. 2015). We analyzed single-unit data recorded during TEBC using either a 500-ms (4 rabbits) or a 1000-ms trace interval (2 rabbits). We treated all recordings as independent because it cannot be determined with certainty that the same cells are recorded from day to day. It is most likely that the brain of a rabbit moves in relation to the recording probe when the rabbit spends time in its home cage, between each recording. After preprocessing, we had 162 well-separated units classified as putative pyramidal cells based on firing rate (2.0 ± 0.16 Hz) and waveform (trough-to-peak latency: 0.68 ± 0.02 ms).

First, responses to the tone-conditioned stimulus were evaluated from a 0.7 s time window starting at the stimulus onset (Figure 3, light grey shading). Almost half of the CA1 pyramidal cells decreased firing (rate decreasing, RD, n = 78, 48.1 %) in response to the stimulus, while less than a quarter (n = 40, 24.7 %) increased firing during the same period of time (rate increasing, RI) and the rest showed no change in firing, i.e. indicated no response (NR, n = 44, 27.2 %). The average overall firing rates and trough-to-peak latencies for the RD cells were 1.57 ± 0.22 Hz and 0.70 ± 0.03 ms, 2.83 ± 0.28 Hz and 0.62 ± 0.04 ms for the RI cells and 2.03 ± 0.33 Hz and 0.68 ± 0.04 ms for the NR cells (see Figure 5A). The difference in overall firing rates between the RD and the RI cells was statistically significant (One-way ANOVA: $F [2, 159] = 5.42$, $p = 0.005$; Bonferroni-corrected post-hoc test, RD vs. RI: $p = 0.004$, 95 % CI [-2.18, -0.33]; RD vs. NR: $p = 0.652$; RI vs. NR: $p = 0.194$) while there was no group difference in the trough-to-peak latencies ($F [2, 159] = 1.16$, $p = 0.316$).

We also analyzed the data separately for each task (trace period 500 ms vs. 1000 ms) and early (less than 50% learned responding) and late (at least 50% learned responding) stages of learning. In the early phase of training using the 500-ms trace period a total of 45 putative pyramidal cells were recorded in 4 animals (8, 4, 22 and 11 per animal) and there were 37.8 % RI cells and 28.9 % RD cells, while the rest were determined NR. In the late

phase of training, the proportions were 5.9 % RI cells and 61.8 % RD cells while the total number of pyramidal cells recorded was 34 (4, 12, 6 and 12 per animal). In the early phase of training using the 1000-ms trace period a total of 67 putative pyramidal cells were recorded in 2 animals (54 and 13 per animal) and there were 23.9 % RI cells and 58.2 % RD cells. In the late phase of training, the proportions were 31.3 % RI cells and 31.3 % RD cells while the total number of pyramidal cells recorded was 16 (8 and 8 per animal). One-way ANOVA indicated a statistically significant difference in overall firing rate between the RI and the RD cells in the early phase of training with the 1000-ms trace period: $F [2, 64] = 3.75$, $p = 0.029$; Bonferroni-corrected post-hoc test, RD vs. RI: $p = 0.028$, 95 % CI [-2.52, -0.11]; RD vs. NR: $p = 1.000$; RI vs. NR: $p = 1.000$. RI cells fired more overall (2.72 Hz ± 0.35 Hz) compared to RD cells (1.40 Hz ± 0.27 Hz). The RI cells also had a narrower spike as indicated by the smaller through-to-peak latency (0.48 ms ± 0.06 ms) compared to the RD cells (0.68 ms ± 0.04 ms) (One-way ANOVA: $F [2, 64] = 3.94$, $p = 0.024$; Bonferroni-corrected post-hoc test, RD vs. RI: $p = 0.029$, 95 % CI [0.02, 0.40]; RD vs. NR: $p = 0.388$; RI vs. NR: $p = 1.000$). In all the other cases there were no statistically significant differences between RI, RD and NR cells in either overall firing rate or trough-to-peak latency.

To summarize, the most common response to the CS was a decrease in firing rate. The cells that did increase firing in response to the CS tended to fire more overall.

Rate decreasing CA1 pyramidal cells devoted a larger proportion of their action potentials to SPW-Rs compared to non-responsive and rate increasing cells

Next, we researched whether the RD, RI and NR cells differed in terms of firing during hippocampal LFP oscillations most often implicated in encoding and consolidation of memories, namely theta and SPW-Rs (Buzsaki 1989, 2015). During SPW-Rs, most pyramidal cells increased firing rate (see example, Figure 4A). This was true regardless of response to the stimulus: RD (n = 61, 78.2 %), RI (n = 33, 82.5 %) and NR (n = 41, 93.2 %).

Overall, the RD cells fired at a rate of 25.31 ± 1.82 Hz, RI cells at a rate of 20.04 ± 0.89 Hz and the NR cells at a rate of 23.60 ± 1.14 Hz during SPW-Rs. There was no difference in firing rate between the cell groups, $F [2, 159] = 2.477$, $p = 0.087$ (Figure 5A). According to the Rayleigh test ($p < 0.001$), 76.9 % (n = 60) of RD cells, 80.0 % (n = 32) of RI cells and 95.5 % (n = 42) of NR cells showed phase-locking to ripple (Figure 4B). Namely, the cells consistently fired during the trough of the ripple-band oscillation (see inset in Figure 4A for an example). Of the ripple phase-locked cells, firing was phase-locked to ripple *trough* specifically in 78.3 % of RD cells, in 71.4 % NR cells and in 62.5 % of RI cells. CA1 pyramidal cells participated in ~40% of SPW-Rs (RD 37.4 ± 3.0 %; RI 40.6 ± 3.7 %; NR 41.3 ± 3.8 %; $F [2, 159] = 0.42$, $p = 0.660$) (Figure 5B). The RD cells fired on average 26.6 ± 2.1 % of their spikes during SPW-Rs, while for the RI cells the corresponding proportion was only 10.4 ± 1.3 and for the NR cells 22.2 ± 2.4 % (Figure 5C). RI cells differed statistically significantly from the RD cells and the NR cells: $F [2, 159] = 14.13$, $p < 0.001$; RD vs. RI: $p < 0.001$, 95 % CI [8.82, 23.62]; NR vs. RI: $p = 0.002$, 95 % CI [3.48, 20.11]; RD vs NR: $p = 0.414$. Separate analyses for subsets of the data based on the two variants of the behavioral task (trace period 500 ms vs. 1000 ms) and on the stage of learning yielded comparable results (details not shown).

To summarize, regardless of responses to the conditioned stimulus, CA1 pyramidal cells were recruited by SPW-Rs and preferentially fired during the ripple troughs. However, RD and NR cells devoted a larger proportion of their overall firing to SPW-Rs than RI cells.

Rate increasing CA1 pyramidal cells fired more often during endogenous hippocampal theta epochs than rate decreasing or non-responsive cells

At last, we examined the firing of RD, RI and NR pyramidal cells during hippocampal theta epochs that took place at least 10 seconds after the CS onset, i.e. reflected endogenous type 2 theta (see Figure 4B): RD pyramidal cells (regardless of SPW-R modulation) fired at a

rate of 2.51 ± 0.20 Hz, RI cells fired at a rate of 4.91 ± 0.79 Hz and the NR cells fired at a rate of 3.13 ± 0.28 Hz. The RI cells differed statistically significantly from the other two groups of cells ($F [2, 159] = 8.87$, $p < 0.001$; RD vs. RI: $p < 0.001$, 95 % CI [-3.79, -1.02]; RD vs. NR: $p = 0.785$; RI vs. NR: $p = 0.019$, 95 % CI [0.22, 3.33]) (see Figure 5A). According to the Rayleigh test ($p < 0.001$), 44.9 % (n = 35) of RD cells, 85.0 % (n = 34) of RI cells and 61.4 % (n = 27) of NR cells showed non-uniform firing during the theta cycle (Figure 4B, inset). Firing tended to center to the trough of the cycle but there was more variation than during ripples. Of the theta phase-locked cells, firing was phase-locked to theta trough (phase preference $\geq ¾ \pi$ or $\leq - ¾ \pi$) specifically in 39.7 % of RD cells, in 36.4 % NR cells and in 67.5 % of RI cells. The RD cells fired during 20.3 ± 2.4 % of all theta epochs and 6.3 ± 0.9 % of their spikes took place during these epochs (Figures 5B and 5C). The RI cells fired during 48.0 ± 2.9 % of all theta epochs and 19.6 ± 1.8 % of their spikes took place during these epochs while the proportions for the NR cells were 34.2 ± 3.8 % and 10.6 ± 1.4 %, respectively. All groups differed from each other in both measures, the proportion of theta epochs that they participated in ($F [2, 159] = 22.85$, $p < 0.001$; RD vs. RI: $p < 0.001$, 95 % CI [-37.73, -17.61]; RD vs. NR: $p = 0.002$, 95 % CI [-23.71, -4.19]; RI vs. NR: $p = 0.011$, 95 % CI [2.41, 25.03]), and in the proportion of spikes that they devoted to the theta epochs ($F [2, 159] = 27.04$, $p < 0.001$; RD vs. RI: $p < 0.001$, 95 % CI [-17.66, -8.92]; RD vs. NR: $p = 0.049$, 95 % CI [-8.50, -0.02]; RI vs. NR: $p < 0.001$, 95 % CI [4.12, 13.94]). Again, separate analyses for subsets of the data based on the two variants of the behavioral task (trace period 500 ms vs. 1000 ms) and on the stage of learning yielded comparable results (details not shown). To summarize, compared to the other two cell types, RI cells fired more often also during spontaneous theta epochs.

Discussion

We studied hippocampal electrophysiological oscillations and CA1 pyramidal cell activity in rabbits subjected to classical trace conditioning of the eyeblink response. Awake SPW-Rs detected during inter-trial intervals of TEBC and those recorded during freely-moving rest were similar. We detected no intrinsic slow rhythmicity in SPW-Rs but half of all SPW-Rs took place in bursts of 2 or more (Oliva et al. 2018; Yamamoto and Tonegawa 2017). External stimulation paced the SPW-Rs so that their occurrence was less likely for a period of up to 10 s after the conditioning trial. Theta epochs showed an opposite pattern, being most abundant right after the training trial. The majority of putative CA1 pyramidal cells either did not change or decreased firing rate in response to the CS (Hattori et al. 2015). Regardless of response profile during TEBC, CA1 pyramidal cells participated in ~40 % of SPW-Rs, during which they fired vigorously (at ~25 Hz). Rate-decreasing cells were most tightly time-locked to ripple troughs. To summarize, SPW-Rs and associated CA1 pyramidal cell activity in rabbits resembles that reported in rats (Ylinen et al. 1995). Surprisingly, a major difference between CA1 pyramidal cells increasing vs. decreasing firing in response to the CS during TEBC was in the firing of these cells during subsequent type 2 theta: Rate increasing cells fired more vigorously also during endogenous theta epochs and their action potentials were more tightly time-locked to the theta trough. The results are discussed in more detail below.

Our first aim was to determine possible differences in awake SPW-Rs based on the behavior of the animal (restrained vs. freely moving) and external environment (TEBC vs. quiet cage). We found that in both situations, SPW-Rs tended to occur at a similar rate (~16 SPW-Rs/min) and manner (~50% single events) (Yamamoto and Tonegawa 2017). SPW-Rs had a slightly faster frequency during awake restrained state than during freely moving rest. This suggests that perhaps CA1 pyramidal cells were more depolarized during restraint. Thus,

perhaps more neurons were recruited to fire action potentials during SPW-Rs that took place between the TEBC trials than during those that took place when the animal was resting. It is possible that synaptic transmission from CA1 to neocortex was also more efficient during SPW-Rs recorded during TEBC sessions. From previous work, we know that SPW-Rs and related neural activity that takes place during the inter-trial intervals are crucial for normal learning of TEBC in rabbits (Nokia et al. 2012a).

Next, we analyzed the intrinsic slow rhythmicity of SPW-Rs using autocorrelation. No statistically significant rhythmicity was found. In rodents, neocortical slow-oscillations modulate the occurrence of SPW-Rs (Headley et al. 2017; Sirota et al. 2003). Further, SPW-R probability is increased during nasal expiration in mice (Liu et al. 2017). There also seems to be an association between bodily rhythms and learning TEBC (Waselius et al. 2018, 2019): Learning is most efficient if trials are targeted to expiration (in humans) or diastole (in rabbits). Our group is currently probing the association between bodily rhythms, hippocampal oscillations, synaptic plasticity and learning both in rodent models and in humans (for recent reviews on the topic, see Heck et al. 2019; Klimesch 2018). Thus, despite the lack of rhythmicity intrinsic to the hippocampus, it is plausible that hippocampal SPW-Rs follow a slow rhythm (< 0.1 Hz) possibly imposed on the hippocampus by bodily oscillations or rhythmic activity elsewhere in the central nervous system (Klimesch 2018; Penttonen and Buzsaki 2003; Penttonen et al. 1999).

In addition to LFPs we also analyzed single-unit activity recorded during the TEBC sessions. In line with previous findings (Hattori et al. 2015), most hippocampal CA1 pyramidal cells showed no change in firing rate or ceased firing in response to the tone used as conditioned stimulus in our current experiment. Interestingly, starting from the first report on place cells (O'Keefe and Dostrovsky 1971) only a small fraction (8/76) of recorded hippocampal principal cells indicate place fields in any given context (see also Thompson

and Best 1989). In addition, for example in the study by MacDonald and colleagues (2011), roughly 30% of putative CA1 pyramidal neurons in rats fired in response to an object or an odor while 53% were active during a ~10-s stimulus-free delay period during which the rat was confined to a small portion of the maze (MacDonald et al. 2011). It is possible that if the subject was exposed to tens or hundreds of different contexts or stimuli, all principal cells near the recording electrode could be labeled "place cells" or "rate increasing cells" based on the emitted action potentials. In any case, it is clear based on current data and previous reports that on any given moment, only a small fraction of CA1 pyramidal neurons is active (Buzsaki 2010). It is worth noting that silence is also a means of contributing towards computation by, for example, improving signal-to-noise ratio within a network (Buzsaki 2010; Hattori et al. 2015). In future studies, the "silent" cells should be studied in detail for example by means of calcium imaging or intracellular recordings that also reveal sub-threshold fluctuations in membrane potential. It might be that even though a cell does not fire an action potential it nonetheless has a significant impact on the surrounding cells by other, non-synaptic means of communication (Jefferys, 1995).

Next, we examined the firing of putative CA1 pyramidal neurons during the stimulus-free inter-trial intervals of TEBC. We hypothesized that rate increasing CA1 pyramidal cells might be the ones "carrying most meaningful information" and might thus be recruited rather than those cells that remained silent or fired more or less randomly during the training trials. Contrary to this, we found that despite the different response profiles during the training trials, both rate decreasing and rate increasing as well as non-responsive cells tended to fire action potentials during SPW-R troughs at comparable rates (Wilson and McNaughton 1994; Ylinen et al. 1995). Based on our current results and a vast literature, it seems that the pattern in which specific groups of cells fire rather than firing rate of individual cells is crucial for the mnemonic function of SPW-Rs (Buzsaki 2015). Unfortunately, due to the low number of

simultaneously recorded pyramidal cells, we were not able to examine patterns of activation from our current data. In future studies, rather than just looking at firing rate, activation patterns of CA1 pyramidal cells during non-spatial training and SPW-Rs should be examined. It might be that what applies during spatial tasks does not directly translate to non-spatial tasks.

Interestingly, during TEBC, the response of the rate decreasing CA1 pyramidal cells seems to last up to a few seconds (Hattori et al. 2015). This corresponds roughly to the duration of the theta-band oscillatory response to the CS evident in hippocampal LFP signal (Figure 2E) (also see for example Nokia et al. 2008). Thus, at last, we also analyzed the firing of putative CA1 pyramidal cells during endogenously emerging epochs of prominent theta oscillations in the hippocampus. We found a clear connection with responding to the CS during TEBC. Rate increasing cells fired action potentials during half of the spontaneous theta epochs, at a frequency of ~5 Hz, while rate decreasing cells participated in only a fifth of the epochs and fired at a rate of ~2.5 Hz. Note that compared to overall firing rate, the rate increasing cells fired roughly twice as often during theta. This implies that the rate increasing cells were more excitable also during type 2 theta elicited in the immobile awake state in rabbits.

During theta, interneurons in the CA1 receive input from the medial septum – diagonal band of Broca (Buzsaki 2002). This rhythmic feed-forward inhibition from local interneurons to the CA1 pyramidal cells could explain the low firing rate of most pyramidal cells during theta generated in response to the CS or endogenously (Klausberger et al. 2003). During theta, CA1 pyramidal cells also receive direct excitatory input as well as disinhibition (i.e. inhibition of inhibitory cells) from the entorhinal cortex (Basu et al. 2016). These entorhinal inputs facilitating firing could be the mechanism by which certain CA1 pyramidal

cells increase firing during theta, whether generated in response to external stimulation or endogenously.

The significance of CA1 pyramidal cell firing during type 2 theta remains to be solved. One option is that the firing of CA1 pyramidal cells during both stimulus-evoked and endogenous type 2 theta is related to reactivation of neural patterns, similar to what has been observed during decision making (vicarious trial and error) in rats performing maze tasks (Johnson and Redish 2007; for a review see Zielinski et al. 2020). This would have to be confirmed in later studies, as, unfortunately, the low number of simultaneously recorded cells excludes the possibility of analyzing firing sequences or assemblies from our current data. Another option is that the increased firing of CA1 pyramidal cells during theta is related to theta-gamma coupling, a phenomenon also suggested to serve memory consolidation in the hippocampo-entorhinal loop (for a review, see Colgin, 2015).

To conclude, CA1 pyramidal cells with various response profiles to the CS during TEBC all fire at a similar rate during SPW-Rs. In comparison, CA1 pyramidal cells responsive to external stimuli preferably fire during spontaneous theta epochs while cells that silence in response to the stimuli do not. These results underline the fact that a decrease in firing rate might be as important as an increase. In addition, the role of endogenous theta epochs in off-line memory consolidation (and not just on-line encoding) should be studied further.

References

Basu J, Zaremba JD, Cheung SK, Hitti FL, Zemelman BV, Losonczy A and Siegelbaum SA. Gating of hippocampal activity, plasticity, and memory by entorhinal cortex long-range inhibition. *Science* 351: 6269: aaa5694, 2016.

Berens P. CircStat: A MATLAB Toolbox for Circular Statistics. 31: 1: 1-21, 2009.

Buzsaki G. Hippocampal sharp waves: their origin and significance. *Brain Res* 398: 2: 242-252, 1986.

Buzsaki G. Two-stage model of memory trace formation: A role for "noisy" brain states. *Neuroscience* 31: 3: 551-570, 1989.

Buzsaki G. Theta oscillations in the hippocampus. *Neuron* 33: 3: 325-340, 2002.

Buzsaki G. Neural syntax: cell assemblies, synapsembles, and readers. *Neuron* 68: 3: 362-385, 2010.

Buzsaki G. Hippocampal sharp wave-ripple: A cognitive biomarker for episodic memory and planning. *Hippocampus* 25: 10: 1073-1188, 2015.

Colgin LL. Theta-gamma coupling in the entorhinal-hippocampal system. *Curr Opin Neurobio* 31: 45-50, 2015.

Foster DJ and Wilson MA. Reverse replay of behavioural sequences in hippocampal place cells during the awake state. *Nature* 440: 7084: 680-683, 2006.

Girardeau G, Benchenane K, Wiener SI, Buzsaki G and Zugaro MB. Selective suppression of hippocampal ripples impairs spatial memory. *Nat Neurosci* 12: 10: 1222-1223, 2009.

Griffin AL, Asaka Y, Darling RD and Berry SD. Theta-contingent trial presentation accelerates learning rate and enhances hippocampal plasticity during trace eyeblink conditioning. *Behav Neurosci* 118: 2: 403-411, 2004.

Hattori S, Chen L, Weiss C and Disterhoft JF. Robust hippocampal responsivity during retrieval of consolidated associative memory. *Hippocampus* 25: 5: 655-669, 2015.

Headley DB, Kanta V and Pare D. Intra- and interregional cortical interactions related to sharp-wave ripples and dentate spikes. *J Neurophysiol* 117: 2: 556-565, 2017.

Heck DH, Kozma R and Kay LM. The rhythm of memory: how breathing shapes memory function. *J Neurophysiol* 122: 2: 563-571, 2019.

Jadhav SP, Kemere C, German PW and Frank LM. Awake Hippocampal Sharp-Wave Ripples Support Spatial Memory. *Science* 336: 1454-1458, 2012.

Jefferys JG. Nonsynaptic modulation of neuronal activity in the brain: electric currents and extracellular ions. *Physiol Rev* 75: 4: 689-723, 1995.

Johnson A and Redish AD. Neural ensembles in CA3 transiently encode paths forward of the animal at a decision point. *J Neurosci* 27: 45: 12176-12189, 2007.

Kim JJ, Clark RE and Thompson RF. Hippocampectomy impairs the memory of recently, but not remotely, acquired trace eyeblink conditioned responses. *Behav Neurosci* 109: 2: 195-203, 1995.

Klausberger T, Magill PJ, Marton LF, Roberts JD, Cobden PM, Buzsaki G and Somogyi P. Brain-state- and cell-type-specific firing of hippocampal interneurons in vivo. *Nature* 421: 6925: 844-848, 2003.

Klimesch W. The frequency architecture of brain and brain body oscillations: an analysis. *Eur J Neurosci* 48: 7: 2431-2453, 2018.

Lisman J, Buzsaki G, Eichenbaum H, Nadel L, Rangananth C and Redish AD. Viewpoints: how the hippocampus contributes to memory, navigation and cognition. *Nat Neurosci* 20: 11: 1434-1447, 2017.

Liu Y, McAfee SS and Heck DH. Hippocampal sharp-wave ripples in awake mice are entrained by respiration. *Sci Rep* 7: 1: 8950, 2017.

Logothetis NK, Eschenko O, Murayama Y, Augath M, Steudel T, Evrard HC, Besserve M and Oeltermann A. Hippocampal-cortical interaction during periods of subcortical silence. *Nature* 491: 7425: 547-553, 2012.

MacDonald CJ, Carrow S, Place R and Eichenbaum H. Distinct hippocampal time cell sequences represent odor memories in immobilized rats. *J Neurosci* 33: 36: 14607-14616, 2013.

MacDonald CJ, Lepage KQ, Eden UT and Eichenbaum H. Hippocampal "time cells" bridge the gap in memory for discontiguous events. *Neuron* 71: 4: 737-749, 2011.

Maingret N, Girardeau G, Todorova R, Goutierre M and Zugaro M. Hippocampo-cortical coupling mediates memory consolidation during sleep. *Nat Neurosci* 19: 7: 959-964, 2016.

Mau W, Sullivan DW, Kinsky NR, Hasselmo ME, Howard MW and Eichenbaum H. The Same Hippocampal CA1 Population Simultaneously Codes Temporal Information over Multiple Timescales. *Curr Biol* 28: 10: 1499-1508.e4, 2018.

Nokia MS, Mikkonen JE, Penttonen M and Wikgren J. Disrupting neural activity related to awake-state sharp wave-ripple complexes prevents hippocampal learning. *Front Behav Neurosci* 6: 84, 2012a.

Nokia MS, Penttonen M, Korhonen T and Wikgren J. Hippocampal theta-band activity and trace eyeblink conditioning in rabbits. *Behav Neurosci* 123: 3: 631-640, 2009.

Nokia MS, Penttonen M, Korhonen T and Wikgren J. Hippocampal theta (3-8Hz) activity during classical eyeblink conditioning in rabbits. *Neurobiol Learn Mem* 90: 1: 62-70, 2008.

Nokia MS, Sisti HM, Choksi MR and Shors TJ. Learning to learn: Theta oscillations predict new learning, which enhances related learning and neurogenesis. *PLOS One* 7: 2: e31375, 2012b.

Nokia MS, Waselius T, Mikkonen JE, Wikgren J and Penttonen M. Phase matters: responding to and learning about peripheral stimuli depends on hippocampal theta phase at stimulus onset. *Learn Mem* 22: 6: 307-317, 2015.

Nokia MS and Wikgren J. Effects of hippocampal state-contingent trial presentation on hippocampus-dependent nonspatial classical conditioning and extinction. *J Neurosci* 34: 17: 6003-6010, 2014.

Novitskaya Y, Sara SJ, Logothetis NK and Eschenko O. Ripple-triggered stimulation of the locus coeruleus during post-learning sleep disrupts ripple/spindle coupling and impairs memory consolidation. *Learn Mem* 23: 5: 238-248, 2016.

O'Keefe J and Dostrovsky J. The hippocampus as a spatial map. Preliminary evidence from unit activity in the freely-moving rat. *Brain Res* 34: 1: 171-175, 1971.

Oliva A, Fernandez-Ruiz A, Buzsaki G, Berenyi A. Role of hippocampal CA2 region in triggering sharp-wave ripples. *Neuron* 91: 6: 1342-1355, 2016.

Oliva A, Fernandez-Ruiz A, Fermino de Oliveira E and Buzsaki G. Origin of gamma frequency power during hippocampal sharp-wave ripples. *Cell Rep* 25: 7: 1693-1700, 2018.

Pastalkova E, Itskov V, Amarasingham A and Buzsaki G. Internally generated cell assembly sequences in the rat hippocampus. *Science* 321: 5894: 1322-1327, 2008.

Penttonen M and Buzsaki G. Natural logarithmic relationship between brain oscillators. *Thalamus & related systems* 2: 145-152, 2003.

Penttonen M, Nurminen N, Miettinen R, Sirvio J, Henze DA, Csicsvari J and Buzsaki G. Ultra-slow oscillation (0.025 Hz) triggers hippocampal afterdischarges in Wistar rats. *Neuroscience* 94: 3: 735-743, 1999.

Ranck JB. Studies on single neurons in dorsal hippocampal formation and septum in unrestrained rats. I. Behavioral correlates and firing repertoires. *Exp Neurol* 41: 2: 461-531, 1973.

Sasaki T, Piatti VC, Hwaun E, Ahmadi S, Lisman JE, Leutgeb S and Leutgeb JK. Dentate network activity is necessary for spatial working memory by supporting CA3 sharp-wave ripple generation and prospective firing of CA3 neurons. *Nat Neurosci* 21: 2: 258-269, 2018.

Scoville WB and Milner B. Loss of recent memory after bilateral hippocampal lesions. *Journal of Neurology, Neurosurgery, and Psychiatry* 20: 11-21, 1957.

Sirota A, Csicsvari J, Buhl D and Buzsaki G. Communication between neocortex and hippocampus during sleep in rodents. *Proc Natl Acad Sci U S A* 100: 4: 2065-2069, 2003.

Takehara K, Kawahara S, Takatsuki K and Kirino Y. Time-limited role of the hippocampus in the memory for trace eyeblink conditioning in mice. *Brain Res* 951: 2: 183-190, 2002.

Tang W, Shin JD, Frank LM and Jadhav SP. Hippocampal-prefrontal reactivation during learning is stronger in awake compared with sleep states. *J Neurosci* 37: 49: 11789-11805, 2017.

Thompson LT and Best PJ. Place cells and silent cells in the hippocampus of freely-behaving rats. *J Neurosci* 9: 7: 2382-2390, 1989.

Waselius T, Wikgren J, Halkola H, Penttonen M and Nokia MS. Learning by heart: cardiac cycle reveals an effective time window for learning. *J Neurophysiol* 120: 2: 830-838, 2018.

Waselius T, Wikgren J, Penttonen M and Nokia MS. Breathe out and learn: Expiration-contingent stimulus presentation facilitates associative learning in trace eyeblink conditioning. *Psychophysiology* e13387, 2019.

Wilson MA and McNaughton BL. Reactivation of hippocampal ensemble memories during sleep. *Science* 265: 5172: 676-679, 1994.

Wu CT, Haggerty D, Kemere C and Ji D. Hippocampal awake replay in fear memory retrieval. *Nat Neurosci* 20: 4: 571-580, 2017.

Yamamoto J and Tonegawa S. Direct medial entorhinal cortex input to hippocampal CA1 is crucial for extended quiet awake replay. *Neuron* 96: 1: 217-227.e4, 2017.

Ylinen A, Bragin A, Nadasdy Z, Jando G, Szabo I, Sik A and Buzsaki G. Sharp wave-associated high-frequency oscillation (200 Hz) in the intact hippocampus: network and intracellular mechanisms. *J Neurosci* 15: 1 Pt 1: 30-46, 1995.

Zielinski MC, Tang W and Jadhav SP. The role of replay and theta sequences in mediating hippocampal-prefrontal interactions for memory and cognition. *Hippocampus* 30: 1: 60-72, 2020.

Legends

Figure 1. Adult female rabbits were trained in trace eyeblink conditioning (TEBC). All rabbits were trained in trace eyeblink conditioning using two different trace intervals. The tone-conditioned stimulus (CS) was separated from the airpuff towards the eye (unconditioned stimulus, US) evoking a blink by either a 500-ms (A) or a 1000-ms (B) trace interval. Sixty trials per session were presented. C) Average (± SEM) learning curves for both tasks. The first three sessions and the session during which a pre-set criterion of 80% learned responses was met (crit) is illustrated along with two sessions preceding it (crit-1, crit-2). Note that for animals that did not meet the learning criterion during the latter task (1000-ms trace interval), the session with the highest percentage of learned responses (and two sessions leading to it) was used for illustration.

Figure 2. Half of SPW-Rs occurred in bursts and SPW-R probability was suppressed by the training trial. A) Example of probe placement in dorsal CA1 after the experiment. Note that the probe has traveled through the pyramidal cell layer (CA1pyr). Scale bar in upper right corner is 0.5 mm. GCL = granule cell layer of the dentate gyrus. B) Example of CA1 LFP signal from an awake restrained rabbit. SPW-Rs were detected by simple thresholding from the signal filtered between 80 and 250 Hz (lower panel). Stars indicate SPW-Rs. C) Distribution of SPW-Rs that took place in isolation (singlet), in bursts of two (doublet), three (triplet) or more (longer). D) Zoom-in on the SPW-R at time 0 s in panel B. E) SPW-R occurrence was paced by the training trials. Namely, the probability of an SPW-R was suppressed for a period of ~10 s after the tone onset. Interestingly, the occurrence of theta epochs was highest immediately following the trial and then reached a plateau. F) SPW-R and theta epoch probability as a function of time elapsed from previous SPW-R and theta epoch, respectively. As evident, data from restrained or rest recordings indicate no innate

slow rhythmicity in SPW-R occurrence or in theta occurrence. In C, E and F bars represent mean and vertical lines depict SEM.

Figure 3. Most CA1 pyramidal cells decreased firing rate in response to the conditioned stimulus (CS, tone) during early (A) and late (B) stages of learning trace eyeblink conditioning. Cells were classified into rate decreasing (top), rate increasing (middle) and non-responsive (bottom) based on the change in firing rate during a 700-ms time period following tone-CS onset (light grey shading). A) Bar plots visualize the grand average response profiles of cells recorded early in learning (less than 50 % learned responses). B) Bar plots visualize the grand average response profiles of cells recorded late in learning (at least 50 % learned responses). US = unconditioned stimulus, air puff toward eye. Each bar graph represents the grand average of the sum of spikes (per 10-ms bin) for all cells in the category. Cells recorded during training with a 500-ms trace period are plotted in black bars and those recorded during training with a 1000-ms trace period are plotted in grey.

Figure 4. CA1 pyramidal cell firing during SPW-Rs (A) was phase-locked to troughs while during theta epochs (B) the cells fired less consistently. A) Representative example of CA1 pyramidal cell firing during SPW-Rs. Raster plot: Spikes are visualized by black dots. Note that for clarity, data is visualized only from SPW-Rs during which this particular pyramidal cell fired at least one spike within 50 ms of the ripple trough. Bar plot in the middle: The sum of spikes (per 1-ms bin) depicted in the raster plot above. Inset: Spikes as a function of ripple phase. Line plot: averaged LFP signal from CA1. B) Representative example of CA1 pyramidal cell firing during theta epochs aligned based on theta trough. Raster plot: Spikes are visualized by black dots. Note that for clarity, data is visualized only from theta epochs during which this particular pyramidal cell fired at least one spike within 500 ms of the theta trough. Bar plot in the middle: The sum of spikes (per 10-ms bin)

depicted in the raster plot above. Inset: Spikes as a function of theta phase. Line plot: averaged LFP signal from CA1.

Figure 5. Regardless of response profile to the conditioned stimulus during trace eyeblink conditioning, CA1 pyramidal cells were equally likely recruited to fire action potentials during SPW-Rs. However, rate increasing cells tended to fire more overall and especially during endogenously generated theta epochs. A) Rate increasing cells had an overall higher firing rate (Hz) compared to rate decreasing cells and they fired more vigorously during theta than rate decreasing or non-responsive cells. All cells fired at comparable rates during SPW-Rs. B) SPW-Rs recruited all CA1 pyramidal cells to fire action potentials to a comparable degree, regardless of how the cells had responded to the conditioned stimulus during trace eyeblink conditioning. Theta oscillations led to action potentials most often in rate increasing cells and least often in rate decreasing cells. C) In line with the low overall firing rate and the low recruitment during theta epochs, rate decreasing cells limited a significant proportion of their activity to SPW-Rs. Similarly, in line with the high baseline firing rate and high recruitment rate during theta oscillations, rate increasing cells fired the largest proportion of their action potentials during theta. Bars represent mean and vertical lines depict SEM. One-way ANOVA and Bonferroni-corrected post-hoc tests were used. Asterisks denote statistical significance: * equals $p < 0.05$, ** equals $p < 0.01$ and *** equals $p < 0.001$. For statistical details, please see Results.

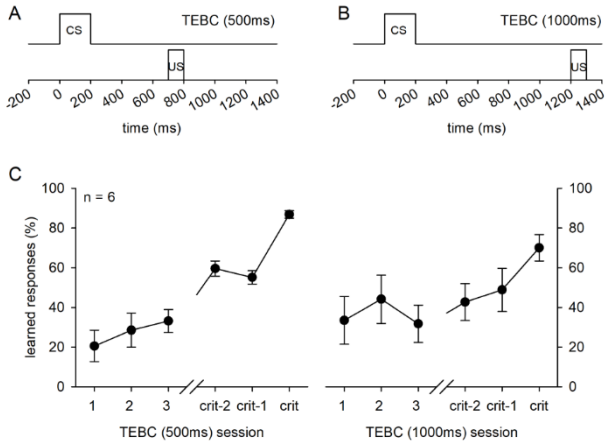
A
CS
TEBC (500ms)
US
-200
0
200
400
600
800
1000
1200
1400
time (ms)
B
CS
TEBC (1000ms)
US
-200
0
200
400
600
800
1000
1200
1400
time (ms)
C
n = 6
learned responses (%)
100
80
60
40
20
0
1
2
3
crit-2
crit-1
crit
TEBC (500ms) session
TEBC (1000ms) session

Figure 1

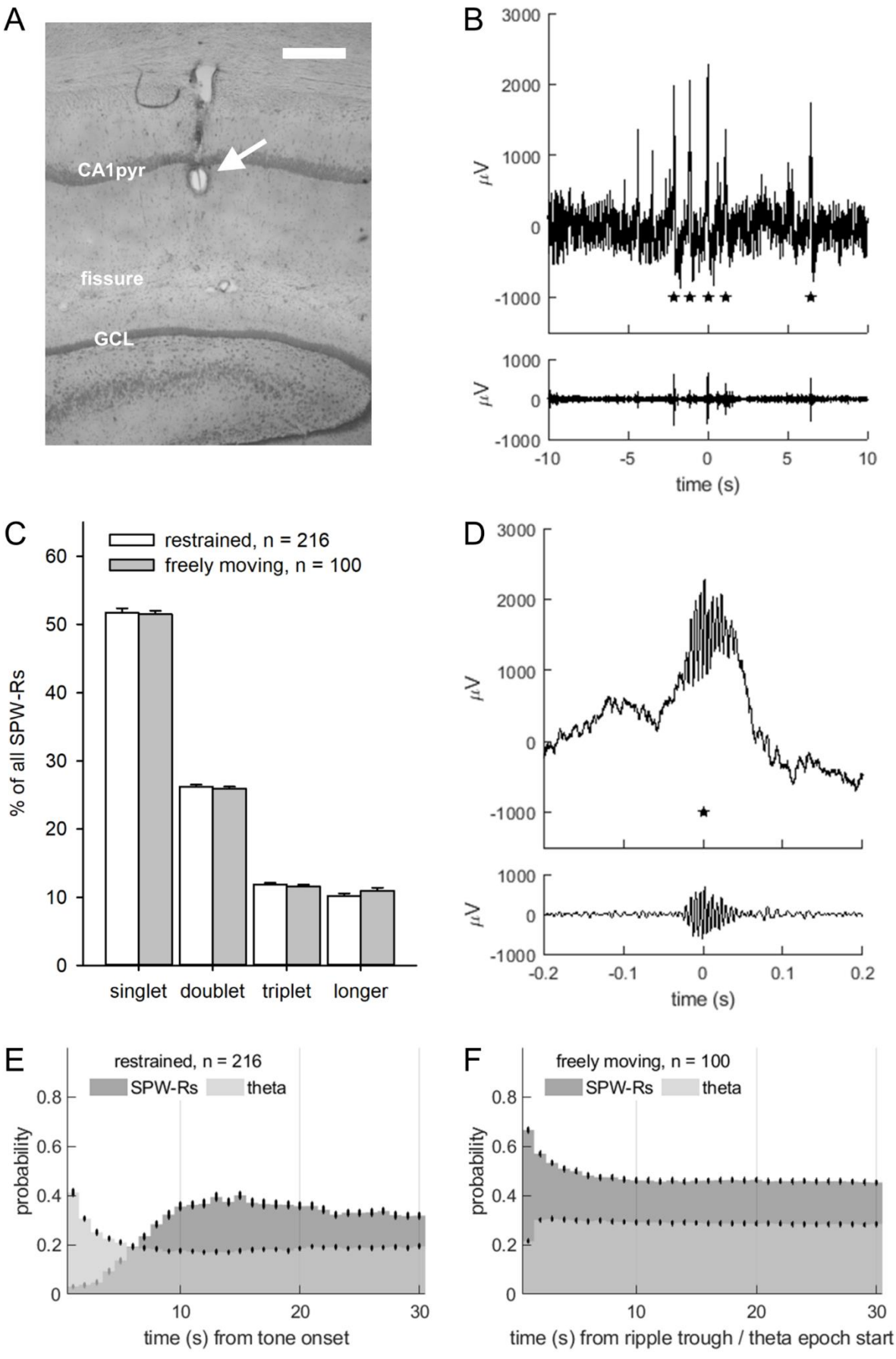
A
CA1pyr
fissure
GCL
B
3000
2000
1000
0
-1000
μV
1000
0
-1000
μV
-10
-5
0
5
10
time (s)
C
restrained, n = 216
freely moving, n = 100
% of all SPW-Rs
60
50
40
30
20
10
0
singlet
doublet
triplet
longer
D
3000
2000
1000
0
-1000
μV
1000
0
-1000
μV
-0.2
-0.1
0
0.1
0.2
time (s)
E
restrained, n = 216
SPW-Rs
theta
probability
0.8
0.6
0.4
0.2
0
10
20
30
time (s) from tone onset
F
freely moving, n = 100
SPW-Rs
theta
probability
0.8
0.6
0.4
0.2
0
10
20
30
time (s) from ripple trough / theta epoch start

Figure 2

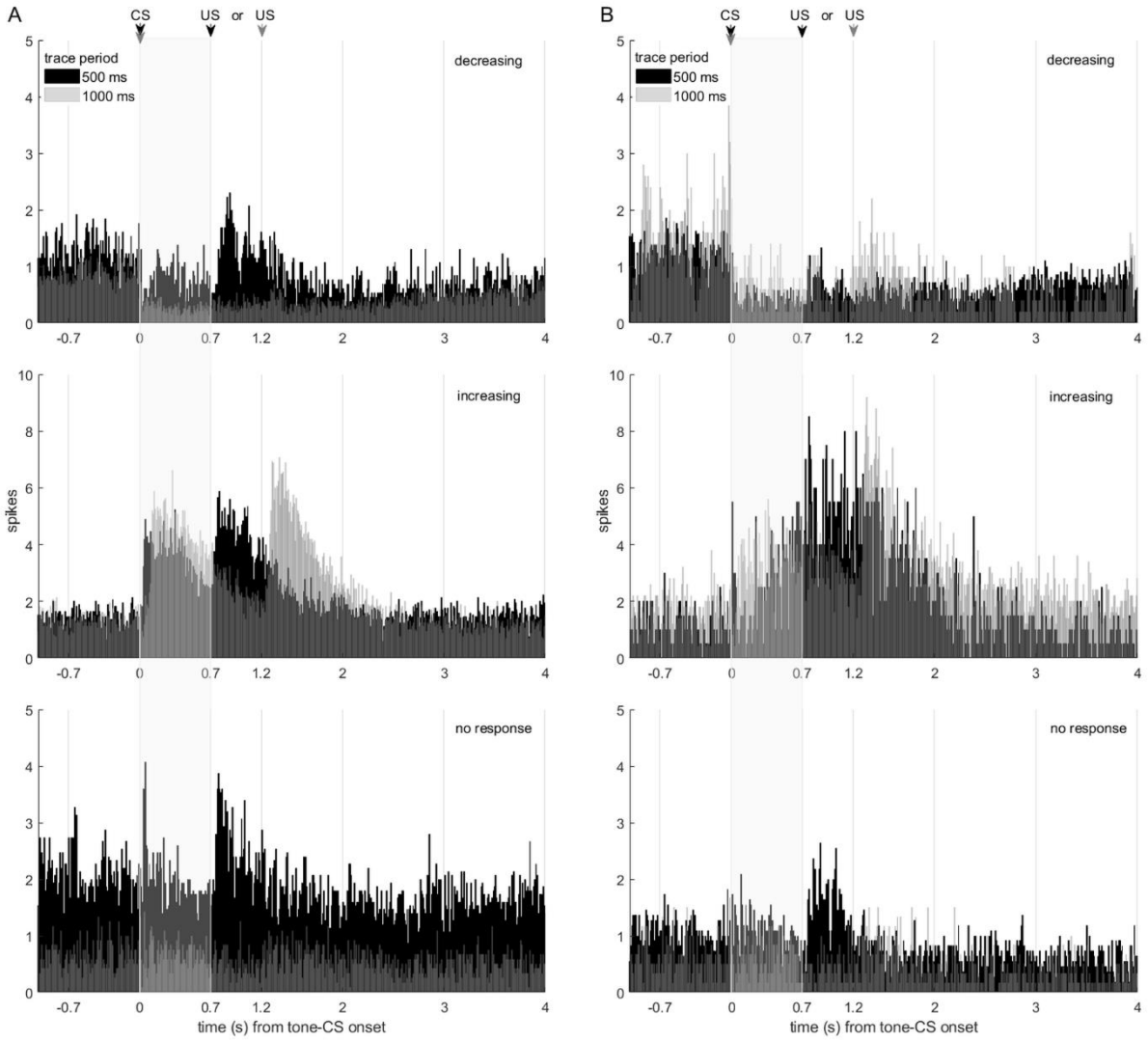
A
B
CS
US or US
trace period
500 ms
1000 ms
decreasing
increasing
no response
spikes
time (s) from tone-CS onset

Figure 3

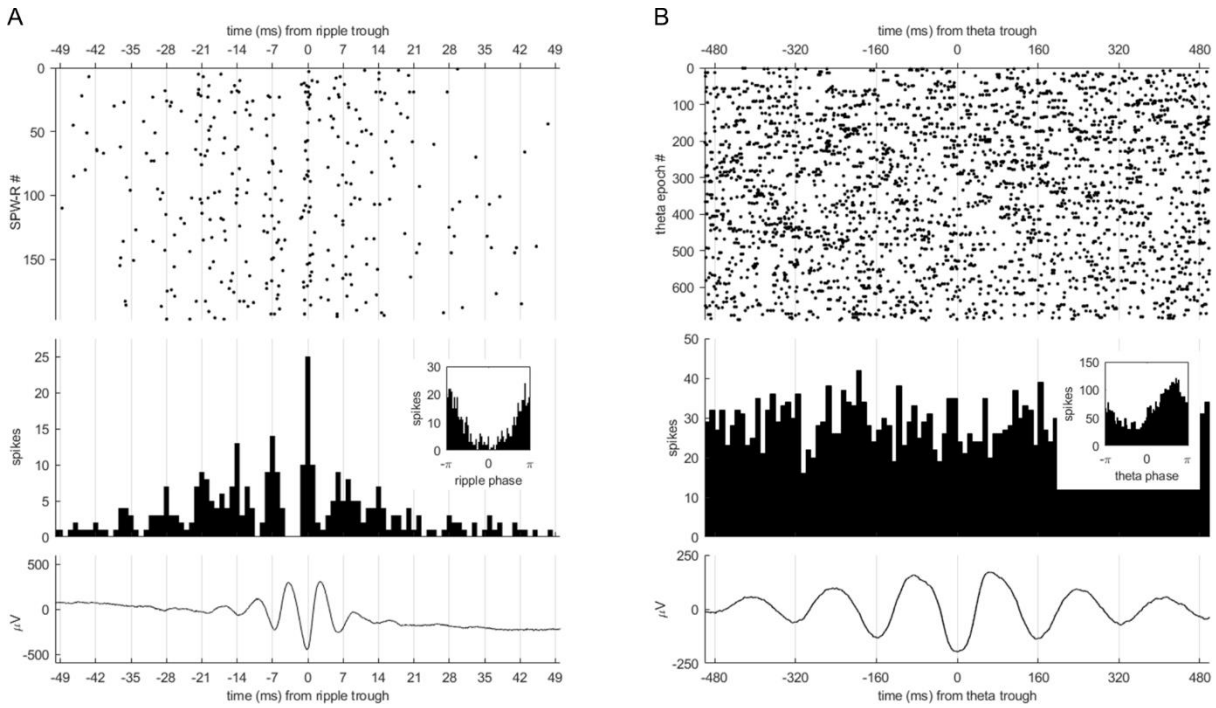
A
time (ms) from ripple trough
SPW-R #
spikes
ripple phase
μV
time (ms) from ripple trough
B
time (ms) from theta trough
theta epoch #
spikes
theta phase
μV
time (ms) from theta trough

Figure 4

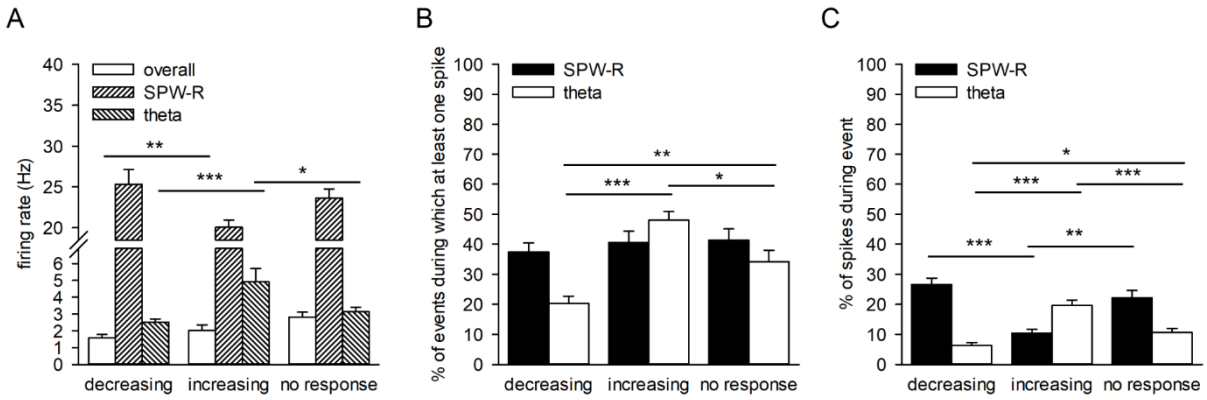
A
B
C
overall
SPW-R
theta
firing rate (Hz)
% of events during which at least one spike
% of spikes during event
decreasing
increasing
no response
**
***
*

Figure 5